Journal of Materials and Environmental Sciences
ISSN : 2028-2508

JMES, 2017 Volume 8, Issue 10, Page 3666-3675

http://www.jmaterenvironsci.com /

Corrosion Control of Mild Steel in Hydrochloric Acid by a 1,5-Benzodiazepine Derivative: Electrochemical and Adsorption studies

J. Sebhaoui[a], M. Boudalia[b], Y. El Bakri[a*], S. Echihi[b,c], I. Rayni[a], A. Ben Ali[b], A. Bellaouchou[b], A. Guenbour[b], M. Tabyaoui[b], A. Zarrouk[d] and E.M. Essassi[a]

[a]Laboratoire de Chimie Organique Hétérocyclique, URAC 21, Pôle de Compétences Pharmacochimie, Université Mohammed V, Faculté des Sciences, Av. Ibn Battouta, BP 1014 Rabat, Maroc.
[b]Laboratory of Materials, Nanotechnology and Environment, Faculty of Sciences, University of Mohammed V Av. Ibn Battouta, BP 1014, Rabat, Morocco.
[c]Laboratory of Water and Environment, Faculty of Sciences, El jadida, BP 20, 24000 El jadida, Morocco.
[d] LC2AME, Faculty of Science, First Mohammed University, PO Box 717, 60 000 Oujda, Morocco.

Received 13 Mar2017,
Revised 29 May 2017,
Accepted 31 May 2017

Keywords
- ✓ Benzodiazepine derivative ;
- ✓ Corrosion inhibition;
- ✓ Mild steel;
- ✓ Hydrochloric acid;
- ✓ Electrochemical impedance spectroscopy.
- ✓ Polarisation curves.

Y. EL Bakri
youness.chimie14@gmail.com
0677288857

Abstract

A new corrosion inhibitor namely, (4Z)-(2-oxopropylidene)-1,2,4,5-tetrahydro-2H-1,5-benzodiazepine-2-one (P1), has been synthesized and its inhibition action on corrosion of mild steel in 1M HCl has been investigated using potentiodynamic polarization and electrochemical impedance spectroscopy (EIS) measurements. The inhibition efficiency for this compound studied increased with the increase in the inhibitor concentrations to attain 96% at the 10^{-3} M of P1. Potentiodynamic polarization study suggests that investigated P1 acts as mixed type inhibitor. EIS study indicates that the P1 forms a protective surface film at metal/electrolyte interface.The adsorption of this compound on steel surface followed Langmuir adsorption isotherm. Kinetic parameters activation were evaluated and discussed from the effect of temperature on corrosion and inhibition processes. The potentiodynamic polarization and electrochemical impedance spectroscopy (EIS) measurements are in good agreement.

I. Introduction:

Organic compounds containing polar groups by which the molecule can become strongly or specifically adsorbed on the metal surface constitute most organic inhibitors [1,2].
These inhibitors, containing heteroatoms particularly N, O and S either in the ring or in the side chain in addition to multiple bonds (double and triple bonds), all forms of aromatic rings and polar functional groups (such as –OH, $–NH_2$, –CN, –SH, NO_2 etc.) act as efficient corrosion inhibitors [3]. Many N-heterocyclic compounds have been proved to be effective inhibitors in acid medium [4-23]. Benzodiazepines have these requirements to act as corrosion inhibitors with maximum degree of unsaturation by virtue of the seven membered ring. A review of literature reveals that though there are large numbers of reports on the synthesis and pharmacological activities of benzodiazepines, only very few works have been carried out on their use as corrosion inhibitors [24-26].
In the present work, the inhibition effect of (4Z)-(2-oxopropylidene)-1,2,4,5-tetrahydro-2H-1,5-benzodiazepine-2-one (P1) on the corrosion of mild steel in 1 M HCl was studied using electrochemical methods. Also, the effect of temperature on the corrosion rate was discussed. Both kinetic and standard thermodynamic parameters

are calculated and discussed in detail. The molecular structure of (4Z)-(2-oxopropylidene)-1,2,4,5-tetrahydro-2H-1,5-benzodiazepine-2-one (P1) is shown in Fig. 1.

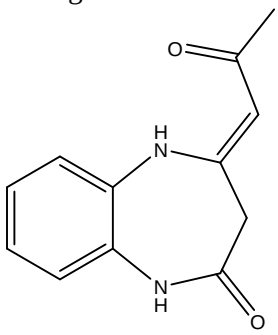

Figure 1: Structure of (4Z)-(2-oxopropylidene)-1,2,4,5-tetrahydro-2H-1,5-benzodiazepine-2-one (P1).

2. Experimental details

2.1. Materials and solutions

Mild steel was used for this study has the following composition: (0.37% C, 0.23%Si, 0.016 S%, 0,68 Mn%, 0.16 Cu%, 0.077Cr%, 0.011Ti%, 0,052Ni%, 0.009 Co% and the remainder iron (Fe))

The steel samples were pre-treated prior to the experiments by grinding with emery paper SiC (120, 600 and 1200); rinsed with distilled water, degreased in acetone in an ultrasonic bath immersion for 5 min, washed again with bidistilled water and then dried at room temperature before use. The acid solutions (1 M HCl) were prepared by dilution of an analytical reagent grade 37 % HCl with doubly distilled water. The concentration range of 3,4-MAT employed was 10^{-6} M to 10^{-3} M.

2.2. Synthesis of the inhibitor:

We took over the reaction of M. El Abbassi et al. [27,28] to synthetize the inhibitor 4Z-(2-oxopropylidene)-1,2,4,5-tetrahydro-2H-1,5-benzodiazepine-2-one **3** from *o*-phenylenediamine **1** and dehydroacetic acid **2.**

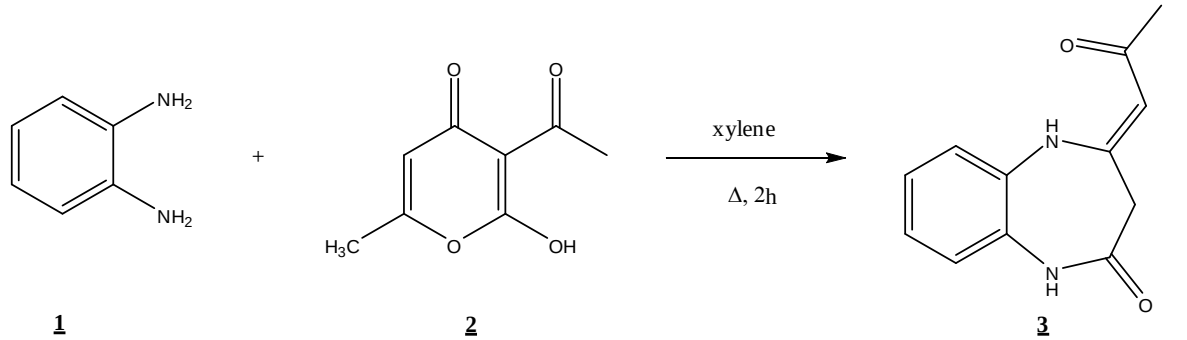

1 **2** **3**

Scheme1: Synthesis of 4Z-(2-oxopropylidene)-1,2,4,5-tetrahydro-2H-1,5-benzodiazepine-2-one (P1).

A mixture of *o*-phenylendiamine **1** (20 mmol) and dehydroacetic acid (10 mmol) **2** in xylene, was refluxed for 2h. After cooling the residue obtained was washed with ethanol to give the compound **3**.

^{1}H-NMR (DMSO-d6): 2,00(s,3H,CH_3) ; 3,00(s,2H ,CH_2) ; 5,20(s,1H,CH) ; 7,10(4$CH_{aromatique}$,m) ; IR(KBr) : 1680, 1610, 1570cm-1; S.M.m/z = 216; mp 230-232°C.

2.3. Potentiodynamic polarization: were carried out in a conventional three-electrode electrolytic cell. Saturated calomel electrode (SCE) and platinum electrode were used as reference and auxiliary electrodes respectively. The working electrode is in the form of a rectangular form from mild steel of the surface 1 cm^2. These electrodes are connected to Volta lab PGZ 301 piloted by computer associated to ‘‘Volta Master 4’’ software. The scan rate was 1 mV/s started from an initial potential of -800 to 0mV/SCE. Before recording each curve, a stabilization time of 30 min was allowed.

2.4.Electrochemical impedance spectroscopy (EIS) :was carried out with the same equipment used for the polarization measurements, sine wave voltage (10 mv peak to peak, at frequencies between 100 kHz and 10 mHz was superimposed on the rest potential. The impedance diagrams are given in the Nyquist representation.

3. Results and discussion

3.1. Polarization study

The polarization curves of mild steel in 1M HCl obtained with and without various concentrations of used inhibitor is shown in Figure 2. Electrochemical kinetic parameters (corrosion potential (E_{corr}), corrosion current density (I_{corr}), cathodic and anodic Tafel slopes (β_c and β_a)), determined from these experiments by extrapolation method [29], are reported in Table 1. The I_{corr} was determined by Tafel extrapolation of only the cathodic polarization curve alone, which usually produces a longer and better defined Tafel region [30]. The I_{corr} values were used to calculate the inhibition efficiency, η_{Tafel}(%), (listed in Table 1), using the following equation [31]:

$$\eta_{Tafel}(\%) = \frac{I_{corr} - I_{corr(i)}}{I_{corr}} \times 100 \qquad (1)$$

where I_{corr} and $I_{corr(i)}$ are the corrosion current densities for steel electrode in the uninhibited and inhibited solutions, respectively.

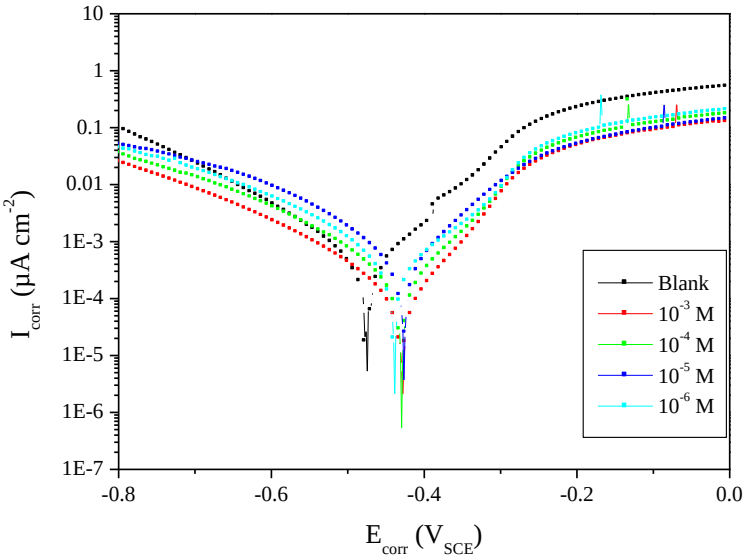

Figure 2: Polarization curves of mild steel in 1M HCl containing different concentrations of P1.

Table 1: Polarization parameters and the corresponding inhibition efficiency for the corrosion of mild steel in 1 M HCl containing different concentrations of (P1) at 303 K.

Medium	Conc (M)	$-E_{corr}$ (mV_{SCE})	β_a ($mV\ dec^{-1}$)	$-\beta_c$ ($mV\ dec^{-1}$)	I_{corr} ($\mu A\ cm^{-2}$)	η_{Tafel} (%)
Blank	—	477	101	138	579	—
P1	10^{-6}	436	99.0	92.0	250	56.0
	10^{-5}	425	75.4	85.6	120	79.2
	10^{-4}	431	78.9	93.8	60	89.0
	10^{-3}	427	68.8	85.0	25	96.0

Inspection of the figure 2 and table 1shows that the addition of this inhibitor has an inhibitive effect in the both anodic and cathodic parts of the polarization curves and generally shifted the E_{corr} value towards the positive direction compared to the uninhibited steel. Thus, addition of this inhibitor reduces the mild steel dissolution as well as retards the hydrogen evolution reaction. In addition, the parallel cathodic Tafel curves in Fig. 2 show that the hydrogen evolution is activation-controlled and the reduction mechanism is not affected by the presence of the inhibitor [32]. So, it could be concluded that (4Z)-(2-oxopropylidene)-1,2,4,5-tetrahydro-2H-1,5-benzodiazepine-2-one is of the mixed-type inhibitor for steel in 1 M HCl solution. Indeed, this inhibitor can exist as a cationic species in 1 M HCl medium, which may be adsorbed on the cathodic sites of the mild steel

and reduce the evolution of hydrogen. Moreover, the adsorption of this compound on anodic sites through the lone pairs of electrons of nitrogen and oxygen atoms will then reduce the anodic dissolution of mild steel.
The analyse of the data in Table 1 revealed that the corrosion current density (I_{corr}) decreases considerably with increasing P1 concentration, with a positive shift in corrosion potential compared to that of uninhibited solution. From the results depicted in Table 1 it is also noted that in presence of P1, the values of both β_a and β_c change irregularly but the change in values of β_c is somewhat more prominent compared to that of β_a suggesting that studied compound act as mixed-type inhibitor. Inspection of these data shows that the addition of P1 inhibits the steel corrosion in 1 M HCl and the protection efficiency increases with C_{inh} reaching its maximum value, 96.0 %, at 10^{-3} M.

3.2 Electrochemical impedance spectroscopy measurements

Figure 3 shows the Nyquist diagrams of mild steel in 1 M HCl solutions containing different concentrations of P1 at 303 K, respectively. All the impedance spectra exhibit single depressed semicircle. The diameter of semicircle increases with the increase of P1 concentration. The semicircular appearance shows that the corrosion of mild steel is controlled by the charge transfer and the presence of P1 does not change the mechanism of mild steel dissolution [33,34]. In addition, these Nyquist diagrams are not perfect semicircles. The deviation of semicircles from perfect circular shape is often referred to the frequency dispersion of interfacial impedance [34-37]. This behaviour is usually attributed to the inhomogeneity of the metal surface arising from surface roughness or interfacial phenomena [33,38], which is typical for solid metal electrodes [39].

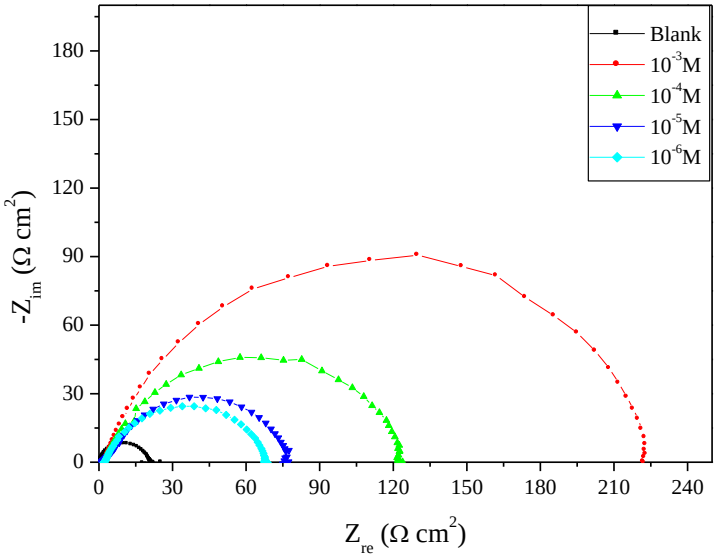

Figure 3: Nyquist plots of mild steel in 1M HCl without and with different concentrations of (P1) at 303 K.

From the impedance data (Table 2), we conclude that the value of R_{ct} increases with increase in concentration of the inhibitor and this indicates an increase in the corrosion inhibition efficiency, which is in concord with the potentiodynamic polarisation results obtained. In acidic solution, the impedance diagrams show perfect semi-circles (Fig. 3) whose size increases with the concentration of the inhibitor indicating a charge-transfer process mainly controlling the corrosion of steel. In fact, the presence of inhibitor enhances the value of the transfer resistance in acidic solution. Values of double layer capacitance are also brought down to the maximum extent in the presence of inhibitor and decrease in the values of C_{dl}. The decrease in C_{dl} is due to the adsorption of this compound on the metal surface leading to the formation of a film from the acidic solution [40].
Values of the double layer capacitance (C_{dl}) were calculated from the frequency at which the impedance imaginary component ($-Z_{im}$) was maximum, using the following equation:

$$f\left(-Z_{im}\right)=\frac{1}{2\pi C_{dl}R_{ct}} \qquad (2)$$

% η_i was calculated using the equation:

$$\eta_i = \left(\frac{R_{ct(inh)} - R_{ct(uninh)}}{R_{ct(inh)}} \right) \times 100 \qquad (3)$$

where $R_{ct(inh)}$ and $R_{ct(uninh)}$ are the charge-transfer resistance values with and without inhibitor, respectively.

Tableau 2: Impedance parameters of mild steel in 1M HCl containing different concentrations of P1 compound at 303 K.

Conc (M)	R_{ct} (Ω cm^2)	f_{max} (Hz)	C_{dl} (μF cm^{-2})	η_i (%)
Blank	21	20	126.31	—
10^{-6}	68	12.5	187.3	69.1
10^{-5}	77	15.8	130.6	72.7
10^{-4}	122	20	65.2	82.7
10^{-3}	223	25	28.5	90.5

3.3. Kinetic-Thermodynamic corrosion parameters

Temperature is an important parameter in studies on metal dissolution. The corrosion rate in acid solutions, for example, increases exponentially with a temperature increase because the hydrogen evolution overpotential decreases [41]. Arrhenius-type dependence is observed between the corrosion rate and temperature. From the Arrhenius plots, the apparent activation energy (E_a) of the corrosion process can be calculated. Some conclusions on the mechanism of the inhibitor action can be obtained by comparing E_a, both in the presence and absence of the corrosion inhibitor. The effect of temperature on the rate of the mild steel corrosion process was studied in 1 M HCl alone and in the presence of 10^{-3} M of P1. The I_{corr} value was obtained by extrapolation of the Tafel lines of experiments carried out at 303, 313, 323 and 333 K. Polarization curves for the mild steel in 1 M HCl solution are shown in Figs. 4 and 5 in two different conditions, without different and with the 10^{-3} M of P1 in the temperature range (303-333 K). The numerical values of the variation of corrosion current density (I_{corr}), corrosion potential (E_{corr}), Inhibitory efficacy (η_{Tafel} (%)), and the degree of surface coverage (θ) at all studied temperatures are given in Table 3. These values were calculated from the intersection of the anodic and cathodic Tafel lines of the polarisation curve at E_{corr}. The inhibition efficiency η_{Tafel} (%) is given by equation 1.

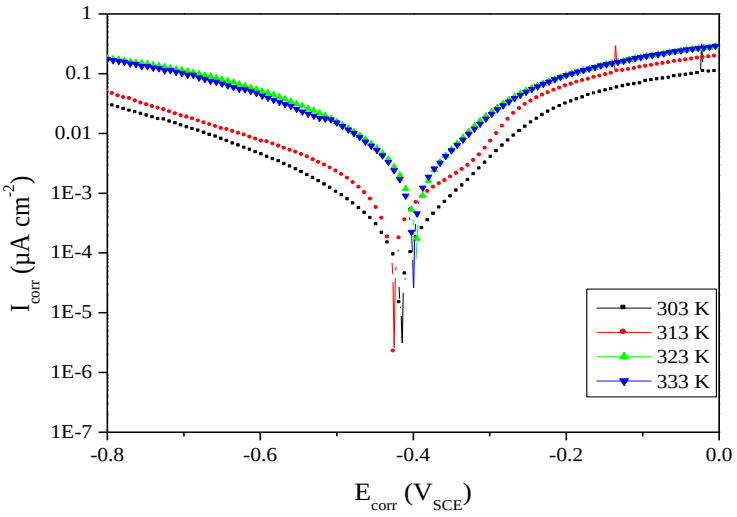

Figure 4: Effect of temperature on the cathodic and anodic responses for steel in 1 M HCl.

In the absence and in the presence of the organic compound, the I_{corr} value increased with increasing temperature. It is seen also that the P1 investigated have been inhibiting properties at all temperatures studied and the values of inhibition efficiency decreases with temperature increase. We were interested in exploring the

activation energy of the corrosion process and the thermodynamics of adsorption of P1. This was accomplished by investigating the temperature dependence of the corrosion current, obtained using Tafel extrapolation method. The corrosion reaction can be regarded as an Arrhenius-type process, the rate is given by

$$I_{corr} = A\exp\left(\frac{-E_a}{RT}\right) \qquad (4)$$

where E_a is the apparent activation corrosion energy, T is the absolute temperature, A is the Arrhenius pre-exponential constant and R is the universal gas constant. This equation can be used to calculate the E_a values of the corrosion reaction without and with P1.

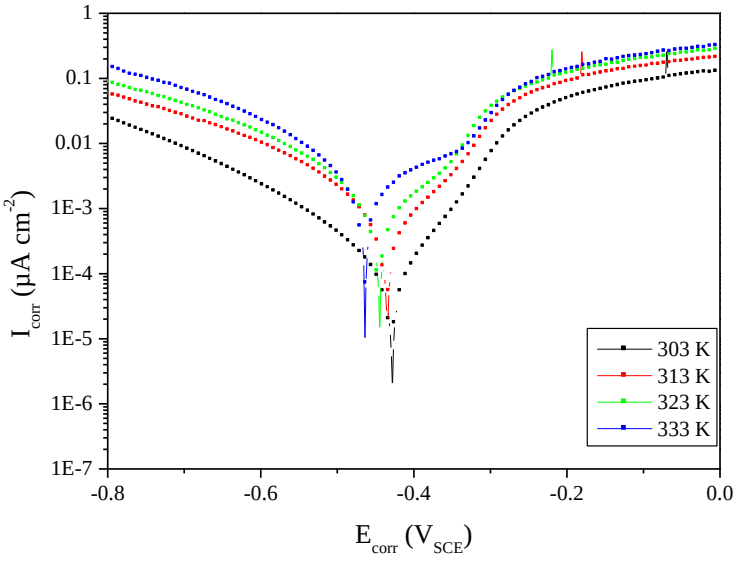

Figure 5: Effect of temperature on the cathodic and anodic responses for steel in 1 M HCl + 10^{-3} M of P1.

Table 3: Electrochemical parameters for corrosion of mild steel in 1M HCl at different temperatures in the absence and presence of 10^{-3} M **P1.**

T (K)	Conc (M)	$-E_{corr}$ (mV_{SCE})	I_{corr} ($\mu A\ cm^{-2}$)	η_{Tafel} (%)
303	Blank		579 .0	
	10^{-3}	413	25.0	96
313	Blank	427	716.1	
	10^{-3}	426	81.0	88
323	Blank	432	2073	
	10^{-3}	398	290.0	86
333	Blank	443	2076	
	10^{-3}	400	577.0	72

Plotting the natural logarithm of the corrosion current density versus 1/T, the activation energy can be calculated from the slope. The temperature dependence of mild steel dissolution in 1 M HCl and in the presence inhibitor is presented in Arrhenius co-ordinates in Fig. 6. The calculated values of the apparent activation corrosion energy in the absence and presence of P1 are listed in the Table 4. All the linear regression coefficients were close to one. The value of E_a found for P1 is higher than that obtained for 1 M HCl solution. The increase in the apparent activation energy may be interpreted as physical adsorption that occurs in the first stage [42]. Szauer and Brand explained that the increase in activation energy can be attributed to an appreciable decrease in the adsorption of the inhibitor on the mild steel surface with increase in temperature. As adsorption decreases more desorption of inhibitor molecules occurs because these two opposite processes are in equilibrium. Due to more desorption of inhibitor molecules at higher temperatures, an important surface of mild steel comes in contact with aggressive environment, resulting increased corrosion rates with increase in temperature [43].

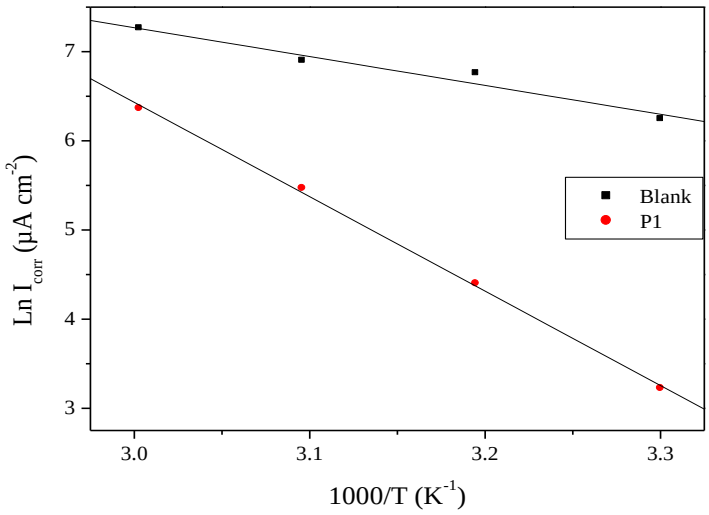

Figure 6: Arrhenius plots for the corrosion of mild steel in 1 M HCl containing 10^{-3} M of P1.

An alternative formulation of Arrhenius equation is [44]

$$I_{corr} = \frac{RT}{Nh}\exp\left(\frac{\Delta S_a}{R}\right)\exp\left(-\frac{\Delta H_a}{RT}\right) \quad (5)$$

where h is Planck's constant, N is Avagadro's number, ΔS_a is the entropy of activation and ΔH_a is the enthalpy of activation. Fig. 7 shows a plot of Ln (I_{corr}/T) vs. 1/T. Straight lines are obtained with a slope of ΔH_a /R and an intercept of Ln R/Nh + ΔS_a /R from which the values of ΔS_a and ΔH_a are calculated and are given in Table 4.

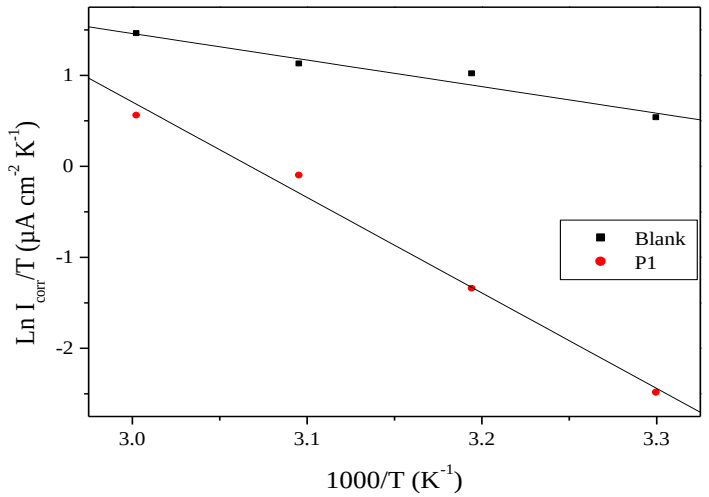

Figure 7: Transition Arrhenius plots for the corrosion of mild steel in 1 M HCl containing 10^{-3} M of P1.

Table 4: The values of activation parameters for steel in 1M HCl in the absence and presence of P1 at 10^{-3} M

Medium	E_a (KJ/mol)	ΔH_a (KJ/mol)	ΔS_a (J/mol K)
Blank	40.5	38	-70.13
P1	88.5	86	70.10

Inspection of these data revealed that the thermodynamic parameters (ΔS_a and ΔH_a) for dissolution reaction of mild steel in 1 M HCl in the presence of inhibitor are higher than that obtained in the absence of inhibitor. The positive sign of ΔH_a reflects the endothermic nature of the mild steel dissolution process suggesting that the dissolution of mild steel is slow [45] in the presence of inhibitor. In the presence of P1, the increase of ΔS_a reveals that an increase in disordering takes place on going from reactants to the activated complex [46].

3.4. Adsorption isotherm and thermodynamic parameters

It is well recognized that the first step in inhibition of metallic corrosion is the adsorption of organic inhibitor molecules at the metal/solution interface and that the adsorption depends on the molecules chemical composition, the temperature and the electrochemical potential at the metal/solution interface. In fact, the solvent H_2O molecules could also adsorb at metal/solution interface. So the adsorption of organic inhibitor molecules from the aqueous solution can be regarded as a quasi-substitution process between the organic compounds in the aqueous phase [Org(sol)] and water molecules at the electrode surface [H_2O (ads)] [47]:

Org (sol) + nH_2O (ads) ↔ Org (ads) + nH_2O (sol)

Where (n) is the size ratio, that is, the number of water molecules replaced by one organic inhibitor. Basic information on the interaction between they inhibitor and the steel surface can be provided by the adsorption isotherm. In order to obtain the isotherm, the linear relation between degree of surface coverage (θ) values (θ= η_{Tafel}% / 100) and inhibitor concentration (C) must be found. Attempts were made to fit the θ values to various isotherms including Langmuir, Temkin and Frumkin. By far the best fit is obtained with the Langmuir isotherm. This model has also been used for other inhibitor systems [48,49]. According to this isotherm, θ is related to C by:

Langmuir: $$\frac{C}{\theta} = \frac{1}{K} + C \qquad (6)$$

where C is the inhibitor concentration, K is the adsorptive equilibrium constant and θ is the surface coverage. Figure 8 shows the plots of C/θ versus C and the expected linear relationship is obtained for this compound. The strong correlation (R^2 = 0.99998 for the compound P1) confirm the validity of this approach.

The constant of adsorption, K_{ads}, is related to the standard free energy of adsorption, ΔG^{o}_{ads}, with the following equation:

$$\Delta G^{o}_{ads} = -RTLn\left(55.5K_{ads}\right) \qquad (7)$$

Where R is the universal gas constant, T is the thermodynamic temperature and the value of 55.5 is the concentration of water in the solution in mol/L.

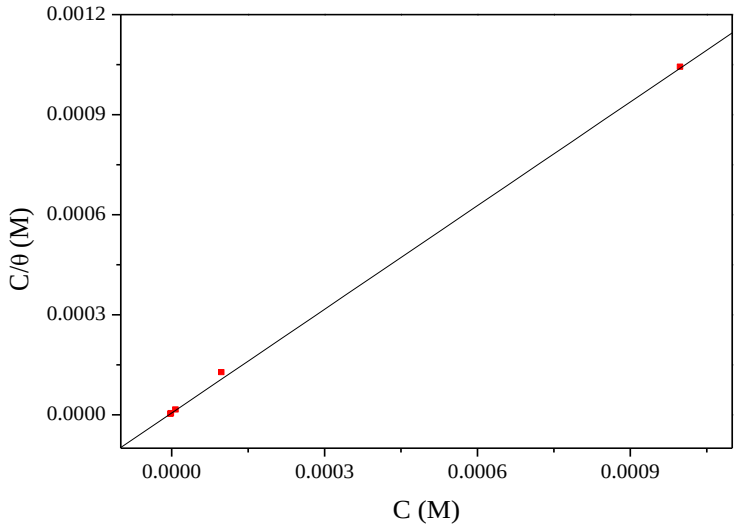

Figure 8: Langmuir isotherm adsorption model of P1 on the surface of mild steel in 1M HCl.

The thermodynamic parameters for the adsorption process were obtained from this figure are shown in Table 5.

Table 5: Thermodynamic parameters for the adsorption of P1 in 1 M HCl on the mild steel at 303K.

	Slope	R^2	K_{ads} (L mol^{-1})	ΔG°_{ads} (KJ/mol)
P1	1.04	0.99998	271814.47	-41.64

Generally, values of ΔG°_{ads} up to -20 kJ mol^{-1} are consistent with the electrostatic interaction between the charged molecules and the charged metal (physical adsorption) while those more negative than -40 kJ mol^{-1} involve sharing or transfer of electrons from the inhibitor molecules to the metal surface to form a coordinate type of bond (chemisorption) [50]. Whereas, the more negative values than -40 kJ mol^{-1} involve charge sharing or transfer from the inhibitor molecules to the metal surface to form a coordinate type of bond (chemisorptions) [17].

Conclusion:

The (4Z)-(2-oxopropylidene)-1,2,4,5-tetrahydro-2H-1,5-benzodiazepine-2-one (P1) is an efficient inhibitor for mild steel in1 M HCl. The inhibition efficiency increases with the addition of inhibitor and reached a maximum of 96 % in the presence of 10^{-3} M of inhibitor. The inhibition efficiency decreases with the increase in temperature. The adsorption of P1 on mild steel obeys Langmuir adsorption isotherm. The inhibitor retards both anodic and cathodic reactions on the surface of the metal. The surface adsorption of the used inhibitor led to a reduction in the double layer capacitance as well as an increase in the charge transfer resistance.

References

1. Damaskin B.B., Pietrij A., Batrokov W.W., *Moskva*, 1968.
2. Okamoto G., Nagayama M., Kato J., Baba T., *Corros. Sci*. 2(1) (1962) 27.
3. Saha S.K., Dutta A., Ghosh P., Sukul D., Banerjee P., *Phys. Chem. Chem. Phys.* 17 (2015) 5690.
4. Nahle A.H., *Corrosion Prevention and Control*, 45(4) (1998) 130.
5. Nahle A., *Bulletin of Electrochemistry*, 18(3) (2002) 110.
6. Ashry E.S.H.E., Nemr A.E., Essawy S.A., Ragab S., *Progress in Organic Coatings*, 61(1) (2008) 20.
7. EL Bakri Y., EL Aoufir Y., Bourazmi H., Harmaoui A., Sebhaoui J., Ben Ali A., Oudda H., Guenbour A., Tabyaoui M., Ramli Y., Essassi E.M., *J. Mater. Environ. Sci. 8(1) (2017) 43.*
8. Boudalia M., Bellaouchou A., Guenbour A., Tabiyaoui M., El Fal M., Ramli Y., Essassi E. M., Elmsellem H., *Mor. J. Chem*. 2(2) (2014) 109.
9. El Bakri Y., Boudalia M., Echihi S., Harmaoui A., Sebhaoui J., Ben Ali A., Ramli Y., Guenbour A., Bellaouchou A., Essassi E.M., *J. Mater. Environ. Sci*. 8(2) (2017) 388.
10. Boudalia M., Sebbar N.K., Bourazmi H., Lahmidi S., Ouzidan Y., Essassi E.M., Tayebi H., Bellaouchou A., Guenbour A., Zarrouk A., *J. Mater. Environ. Sci*. 7(3) (2016) 888.
11. Granese S.L., Rosales B.M., Oviedo C., and Zerbino J.O., *Corros. Sci.* 33(9) (1992) 1439–1453.
12. Nahle A., *Bulletin of Electrochemistry*, 21(6) (2005) 281.
13. Raicheva S. N., Aleksiev B. V., Sokolova E.I., *Corros. Sci*. 34(2) (1993) 350.
14. Nahle A., Abu-Abdoun I., and Abdel-Rahman I., *Anti-Corrosion Methods and Materials*, 54(4) (2007) 248.
15. Ghazoui A., Zarrouk A., Bencaht N., Salghi R., Assouag M., El Hezzat M., Guenbour A., Hammouti B., *J. Chem. Pharm. Res*. 6 (2014) 704.
16. Zarrok H., Zarrouk A., Salghi R., Ramli Y., Hammouti B., Al-Deyab S.S., Essassi E.M., Oudda H., *Int. J. Electrochem. Sci*. 7 (9) (2012) 8958.
17. Bendaha H., Zarrouk A., Aouniti A., Hammouti B., El Kadiri S., Salghi R., Touzan R., *Phys. Chem. News* 64 (2012) 95.
18. Zarrouk A., Hammouti B., Zarrok H., Salghi R., Dafali A., Bazzi L., Bammou L., Al-Deyab S.S., *Der Pharm. Chem*. 4(1) (2012) 337.
19. Ghazoui A., Saddik R., Benchat N., Hammouti B., Guenbour M., Zarrouk A., Ramdani M., *Der Pharm. Chem*. 4(1) (2012) 352.
20. Zarrouk A., Hammouti B., Zarrok H., Bouachrine M., Khaled K.F., Al-Deyab S.S., *Int. J. Electrochem. Sci*. 6 (2012) 89.

21. Zarrok H., Zarrouk A., Salghi R., Assouag M., Hammouti B., Oudda H., Boukhris S., Al Deyab S.S., Warad I., *Der Pharm. Lett*. 5 (2013) 43.
22. Zarrok H., Saddik R., Oudda H., Hammouti B., El Midaoui A., Zarrouk A., Benchat N., Ebn Touhami M., *Der Pharm. Chem*. 3(5) (2011) 272.
23. Zarrouk A., Hammouti B., Touzani R., Al-Deyab S.S., Zertoubi M., Dafali A., Elkadiri S., *Int. J. Electrochem. Sci*. 6(10) (2011) 4939.
24. Niouri W., Zerga B., Sfaira M., Taleb M., Hammouti B., Ebn Touhami M., AlDeyab S.S., Benzeid H., Essassi E.M., *Int. J. Electrochem. Sci.* 7 (2012) 10204.
25. El Aoufir Y., Sebhaoui J., Lgaz H., El Bakri Y., Zarrouk A., Bentiss F., Guenbour A., Essassi E.M., Oudda H., *J. Mater. Environ. Sci*. 8(6) (2017) 2173.
26. Laabaissi T., Bouassiria M., Oudda H., Zarrok H., Zarrouk A., A. Elmidaoui, Lakhrissi L., Lakhrissi B., Essassi E.M., Touir R., *J. Mater. Environ. Sci.* 7 (2016) 1548.
27. Abbassi M.E., Essassi E.M., and Fifani J., *Tetrahedron Letters*. 28(l3) (1987**)** 1392.
28. Abbassi M.E., Djerrari B., Essassi E.M., and Fifani J., *Tetrahedron Letters*. 30 (50) (1989) 7070.
29. Lebrini M., Bentiss F., Chihib N., Jama C., Hornez J.P., Lagrenée M., *Corros. Sci.* 50 (2008) 2914.
30. McCafferty E., *Corros. Sci.* 47 (2005) 3202.
31. Bouklah M., Benchat N., Aouniti A., Hammouti B., Benkaddour M., Lagrenée M., Vezin H., Bentiss F., *Prog. Org. Coat.* 51 (2004) 124.
32. Bentiss F., Jama C., Mernari B., El Attari H., El Kadi L., Lebrini M., Traisnel M., Lagrenée M., *Corros. Sci.* 51 (2009) 1635.
33. Mansfeld F., Kendig M.W., Tsai S., *Corrosion* 38 (11) (1982) 580.
34. Shih H., Mansfeld F., *Corros. Sci*. 29 (1989) 1240.
35. Martinez S., Metikoš-Huković M., *J. Appl. Electrochem*. 33 (2003) 1142.
36. Bentiss F., Lebrini M., Vezin H., Chai F., Traisnel M., Lagrené M., *Corros. Sci*. 51 (2009) 2165.
37. Danaee I., Noori S., *Int. J. Hydrog. Energy*. 36 (2011) 12102.
38. Larabi L., Harek Y., Traianel M., Mansri A., *J. Appl. Electrochem*. 34 (2004) 833.
39. Aramaki K., Hagiwara M., Nishihara H., *Corros. Sci*. 5 (1987) 487.
40. Bentiss F., Largrenee M., Traisenl M., Hornez J.C., *Corros. Sci*. 41 (1999) 789.
41. Popova A., Sokolova E., Raicheva S., Christov M., *Corros. Sci.* 45 (2003) 33.
42. Martinez S., Stern I., *Appl. Surf. Sci*. 199 (2002) 83.
43. Szauer T., Brand A., *Electrochim. Acta*. 26 (1981) 1219.
44. Bochris J.O'M., Reddy A.K.N., *Modern Electrochemistry*, vol. 2, *Plenum Press, New York*, (1977).
45. Guan N.M., Xueming L., Fei L., *Mater. Chem. Phys*. 86 (2004) 59.
46. Khamis E., Hosney A., El-Khodary S., *Afinidad* 52 (1995) 102.
47. Do D., Adsorption Analysis: Equilibria and Kinetics, vol.2, *Imperial College Press*, (1980)**.**
48. Kosec T., Milošev I., Pihlar B., *Appl. Surf. Sci*. 253 (2007) 8863-8873.
49. Mehaute A.H., Grepy G., *Solid State Ionics* 9(10) (1983) 30.
50. Bensajjay F., Alehyen, S., El-Achouri, M. S., Kertit S., *Anti-Corros. Methods Mater*. 50 (*2003)* 409.